A Palm-Sized Omnidirectional Mobile Robot Driven by 2-DOF Torus Wheels

Yunosuke Sato[1], Ayato Kanada[2], and Tomoaki Mashimo[3]

***Abstract*— This paper proposes a palm-sized omnidirectional mobile robot with two torus wheels. A single torus wheel is made of an elastic elongated coil spring in which the two ends of the coil connected each other and is driven by a piezoelectric actuator (stator) that can generate 2-degrees-of-freedom (axial and angular) motions. The stator converts its thrust force and torque into longitudinal and meridian motions of the torus wheel, respectively, making the torus work as an omnidirectional wheel on a plane. In this paper, we build a control system of a piezo-driven 2-degrees-of-freedom torus wheel and evaluate its performance measures, such as the transient characteristics, the orientation accuracy and the payload capacity. An omnidirectional robot with the two torus wheels is constructed, and the feedback control for a desired planar motion is demonstrated. The design inspired by a ring torus represents the possibility toward the creation of an unprecedentedly simple, light, and compact 2-wheel omnidirectional robot.**

I. INTRODUCTION

In geometry, a torus (colloquially donut) is a surface formed by rotating a circle around an axis orthogonal to the circle in three-dimensional space. Such geometric structures are not found in conventional machines but are frequent in nature. Several creatures with a structure related to the torus have provided an inspiration for us to design new robots. Nemerteans have cylindrical, sleeve-like proboscis that can evert the outward to increase its length for predation and locomotion [1]. Sea anemones with soft torus bodies have an outer skin that inverts inward to squeeze and envelop their prey [2]. Robots using these eversion/inversion mechanisms have been proposed for applications in various areas, such as search and rescue, grasping, and the inspection of inaccessible places where existing robots cannot go [1]–[5].

Mobile robots that carry parts and boxes in factories and warehouses are required to move in designated directions on the floor quickly and efficiently. To move a lateral direction, conventional vehicles uses steering to achieve a desired posture, but it is time-consuming and needs a space. Approaches to address this issue is the use of omnidirectional robots that can move in any direction [6]–[9]. The most common omnidirectional traveling mechanism is the omni wheel, which have small free rollers around the circumference that is perpendicular to the turning direction [10]–[14]. The direction of omni mobile robots is determined by the composition of the vector force that three or four wheels generate. Unfortunately, when a wheel idles, the omniwheel system goes out of control. To solve this problem, traveling mechanisms that can actively move in a designated direction by a single wheel unit have been proposed [15]–[23]. However, the omnidirectional mechanisms with multiple actuators complicate and enlarge the wheel systems.

A ring torus is able to function as an omnidirectional wheel with 2 degrees of freedom (DOF): the large circle (longitudinal) direction and the small circle (meridian) direction, as shown in Fig. 1. The simplicity of the torus wheel would

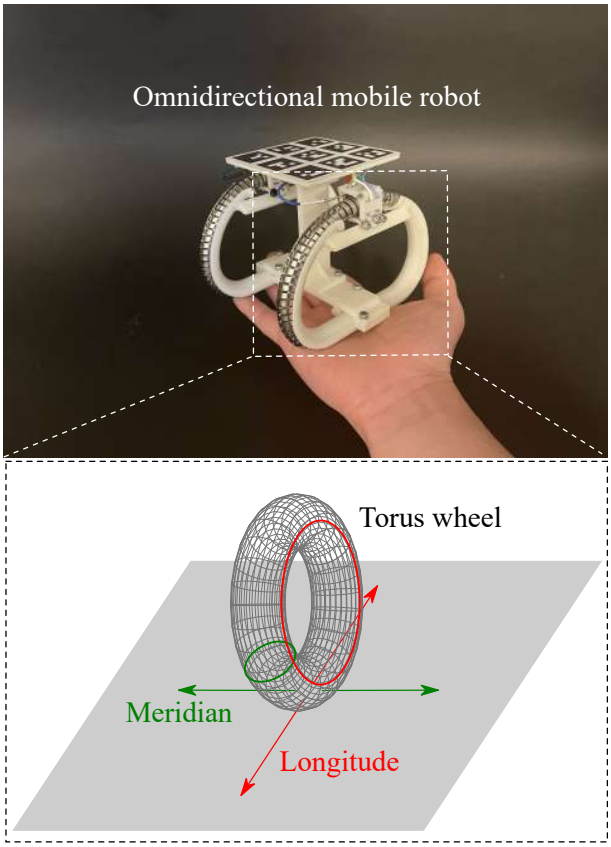

Fig. 1. The concept of the torus wheel. The rotation in the meridian direction of the torus wheel moves left and right, and the rotation in the londitude moves back and forth.

This paper was recommended for publication by Editor Cecilia Laschi upon evaluation of the Associate Editor and Reviewers' comments. This work was supported in part by NSK Foundation for Advancement of Mechatronics *(Corresponding author: Ayato Kanada)*

[1]Yunosuke Sato is with the Department of Mechanical Engineering at Toyohashi University of Technology, 1-1 Hibarigaoka, Tempaku-cho, Toyohashi, Aichi, 441-8580, Japan sato.yunosuke.vf@tut.jp

[2]Ayato Kanada is with the Department of Mechanical Engineering at Kyushu University, 744 Motooka, Nishi-ku, Fukuoka, 819-0395, Japan kanada@mech.kyushu-u.ac.jp

[3]Tomoaki Mashimo is with the Graduate School of Natural Science and Technology at Okayama University, 3-1-1 Tsushimanaka, Kita-ku, Okayama, 700-8530, Japan mashimo@okayama-u.ac.jp

be advantageous to miniaturize of omnidirectional mobile robots because it could reduce components. However, the key is how to realize the torus wheel with an appropriate flexibility. Rotating the torus wheel in the longitudinal direction is probable, but the rotation in the meridian direction requires a sufficient flexibility of the whole torus, unlike rubber tires. Furthermore, an actuation mechanism that transfers its driving force into the torus is essential.

A design concept of multiple DOF actuators is to reduce the number of motors and transmissions and facilitate the miniaturization of the systems. We have studied a piezoelectric actuator with multiple DOF. (It was called flexible ultrasonic motor in [24], [25].) This motor consists of a single cubic stator with an elastic elongated coil spring threaded through the stator hole. When voltages are applied to piezoelectric elements on the stator, the coil spring can selectively move axial and angular motions. We employ this actuator to drive the torus wheel for the sake of the simplicity and small size. A single torus wheel is made of an elastic elongated coil spring in which the two ends of the coil connected each other, as shown in Fig. 2. The stator of the piezoelectric actuator converts its thrust force and torque into longitudinal and meridian motions of the torus wheel, respectively, making the torus work as an omnidirectional wheel. In the past, similar concepts were shown in patents [26], [27] but the mechanisms use many friction tires or gears to transmit meridian rotation. The novelty of this study is that the torus wheel consists of a single coil spring, and the robot using the two-torus wheel enables the omnidirectional movement with a minimum number of components.

The rest of this paper is organized as follows. Section II explains the principle and design of the torus wheel. We evaluate the basic characteristics of the wheel system, such as velocity, payload capacity, linearity, and omnidirectional drivability in section III. In section IV, we build a robot with the two torus wheels and demonstrate a point-to-point movement under P control and a step climbing test.

II. Design and Fabrication

A. Omnidirectional Torus Wheel

Let us explain the design of an omnidirectional torus wheel driven by a piezoelectric actuator (stator), as shown in Fig. 2. The stator is a phosphor bronze cube with a side length of 14 mm, a center hole of 10 mm in diameter, and eight piezo elements adhered on the sides. The piezoelectric elements have a length of 14 mm, a width of 10 mm, and a thickness of 0.5 mm and have two silver electrodes on the outer side. The torus wheel is made of an elastic elongated coil spring in which the two ends of the coil connected each other. The coil spring is a stainless wire formed into a right-hand helix with a length of 300 mm, a width of 3 mm, and a thickness of 0.15 mm. When the stator generates a thrust force and torque, the torus wheel rotates in the longitudinal and meridian directions, respectively.

In our design, the coil spring has a role for not only the torus wheel but also for a pre-pressure mechanism [24]. The pre-pressure acting on the inner surface of the stator produces

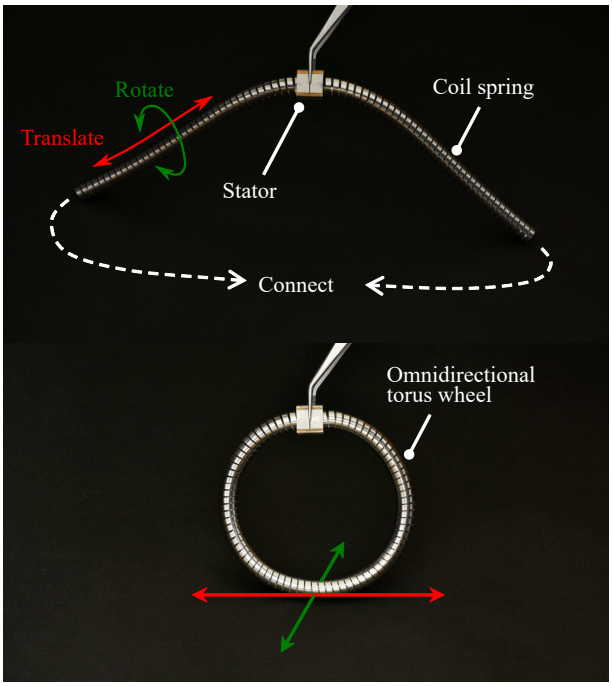

Fig. 2. The omnidirectional torus wheel is created by connecting the two ends of a flexible coil spring.

an optimal contact force on the stator-spring interface to enhance the thrust force and the torque. To provide this contact force constantly, we design the coil spring to have a slightly larger diameter than the stator hole through which it passes. In other words, the restoring force of the coil maintains the optimal pre-pressure.

B. Driving Principle

As the driving principle, the stator excites different vibration modes for generating a thrust force and torque. The thrust force is generated by coupling the first extension mode (Mode 1) and the second extension mode (Mode 2) of the stator shown in Fig. 3(a). Mode 1 is a vibration that repeats expansion and contraction symmetrically. Mode 2 is a vibration that expands the stator edge asymmetrically about the axial direction. When both vibration modes are excited simultaneously at the same resonance frequency, the stator produces an elliptical motion shown in Fig. 3(b). This elliptical motion transfers a thrust force to the coil spring by friction. When two voltages are applied to the piezoelectric elements (Fig. 3(c)), both modes are excited at the same driving frequency. These voltages are expressed as

$$\begin{aligned} E_1 &= A_e(\sin(2\pi f_e t)) \\ E_2 &= A_e(\sin(2\pi f_e t + \phi)) \end{aligned} \quad (1)$$

where A_e and f_e are the amplitude and the frequency of the voltages, respectively, and ϕ is the phase between the two voltages. We set $A_e = 120$ [V_{p-p}] and $f_e = 81.5$ [kHz] for the thrust force. The coil moves forward when the phase is set to $\phi = \pi/2$, and backward when $\phi = -\pi/2$.

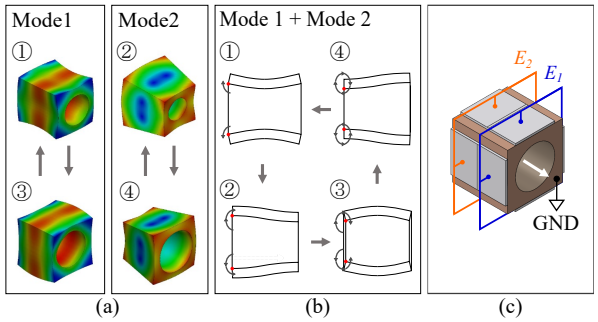

Fig. 3. Driving principle of the piezoelectric actuator that generates a thrust force. (a) Two vibration modes (Mode 1 and Mode 2) generated by stator. (b) When T1 and T2 modes are simultaneously excited, the stator generates an elliptical motion. (c) Applied voltages for the motor. The arrow means the resulting thrust force.

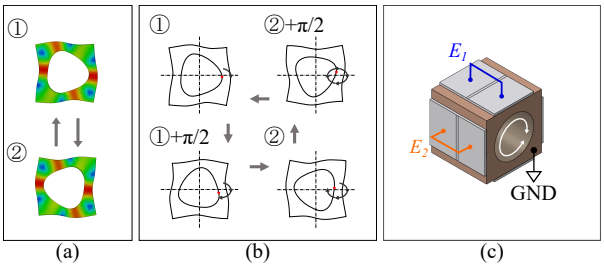

Fig. 4. Driving principle of the piezoelectric actuator that generates a torque. (a) Three-wave vibration mode generated by stator. (b) When three-wave vibration modes with a wavelength difference of $\pi/2$ along the circumference are simultaneously excited, the stator generates an elliptical motion. (c) Applied voltages for the motor. The arrow means the resulting torque.

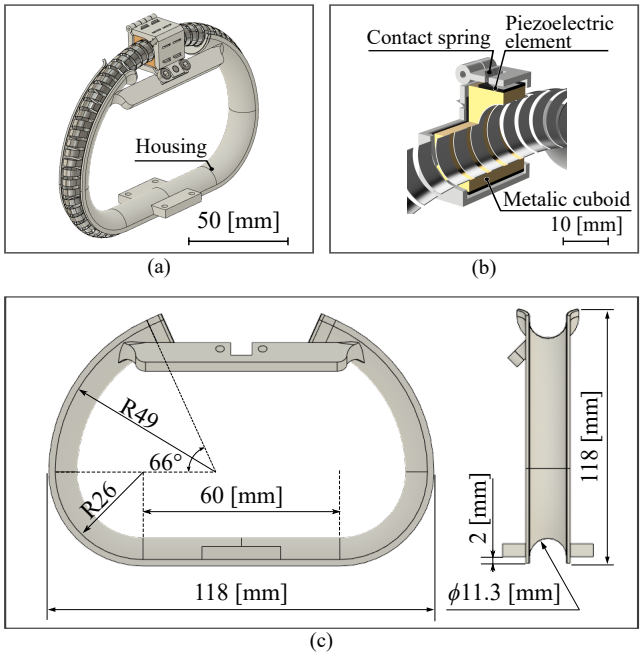

Fig. 5. (a) Housing and electrodes for the torus wheel. (b) Springs provide electrical contacts to the stator. (c) The housing holds the coil spring.

TABLE I

COMPARISON OF HOLONOMIC SINGLE WHEEL UNITS

Ref.	Size [mm]	Mass [kg]	Type
[16]	H:104 W:104 D:359	3.05	Omni-crawler
[22]	H:360 W:220 D:220	1.5	Balancing ball
[23]	H:120 W:120 D:120	1.6	Spherical outer shell
Proposed	H:118 W:20 D:118	0.066	Flexible torus wheel

The torque is generated by coupling a vibration mode that excites three waves along the circumference and another three-wave mode with a wavelength difference of $\pi/2$ along the circumference (Fig. 4(a)). When these three-wave vibration modes are simultaneously excited, the stator generates an elliptical motion and the resulting torque, as shown in Fig. 4(b). When two voltages E_1 and E_2 are applied to the piezoelectric elements (Fig. 4(c)), both modes are excited at the same driving frequency. We set $A_e = 120$ [V_{p-p}] and $f_e = 73.0$ [kHz] for the torque generation. The direction of the torque is selected by changing the phase to $\phi = \pi/2$ or $\phi = -\pi/2$.

C. Housing

We design a housing (Fig. 5(a)) to maintain the shape of the torus wheel because the coil spring is too flexible. It consists of two parts: the part that supplies electric power to the stator (Fig. 5(b)) and the part that keeps the wheel in the desired shape (Fig. 5(c)). The power supply part has contact springs to which eight wires are connected. When the stator is inserted into the part, these springs are elastically deformed and contacted with each piezoelectric element, making electricity flow for driving. The holding part has a semicircular cross-section to support the torus wheel, and its entire shape is like a deformed circle. In Fig. 5(c), the reason of employing the straight shape at the bottom that contacts the ground is to stabilize the motion of the 2-wheeled robot shown in section IV. The inside of the semicircular cross-section has polyethylene tape to reduce friction with the wheel. The total weight of the wheel and housing is 66 g. Our prototype is relatively small and lightweight compared to conventional holonomic single-wheel units shown in Table I.

D. Determination of Traveling Direction

We define a control method for diagonal movement of the torus wheel. A technical problem in the control system is that applying the voltages simultaneously for longitudinal and meridian motions is difficult because their resonant frequencies are different. To avoid this problem, we implement a program to divide the driving time into two parts, one for the longitudinal direction T_l and the other for the meridian direction T_m, in one control cycle time T = 50 ms. Fig. 6 shows how to determine the traveling direction of the torus wheel by the ratio of T_l and T_m. Assuming that the driving velocities V_l and V_m are proportional to the driving time T_l and T_m, we obtain

$$\begin{bmatrix} V_l \\ V_m \end{bmatrix} = \frac{1}{T} \begin{bmatrix} T_l V_{l\_steady} \\ T_m V_{m\_steady} \end{bmatrix} \quad (2)$$

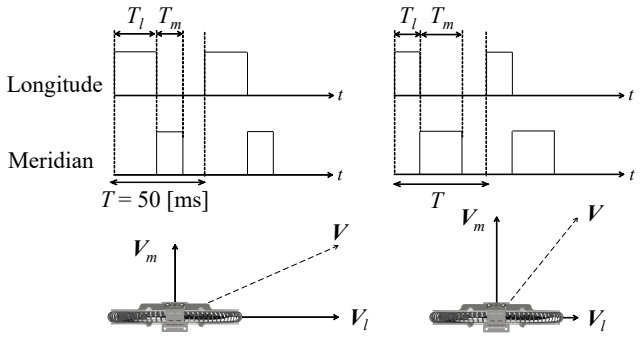

Fig. 6. Time table of the control cycle for diagonal movement. The direction of the torus wheel is determined by the ratio of T_l and T_m.

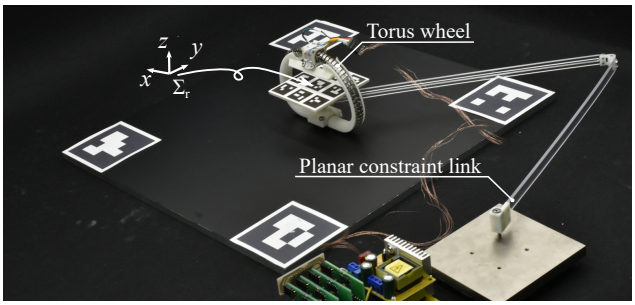

Fig. 7. Experimental setup to measure the position and velocity of the torus wheel.

where V_{l_steady} and V_{m_steady} are the steady-state driving velocity. When we consider $\boldsymbol{V}_l$ and $\boldsymbol{V}_m$ as velocity vectors, the velocity vector of the torus wheel $\boldsymbol{V}$ is expressed as

$$\boldsymbol{V} = \boldsymbol{V}_l + \boldsymbol{V}_m \tag{3}$$

We manipulate the driving times T_l and T_m to control the traveling direction of the torus wheel in the experiments. Note that the amplitude, frequency, and phase of the voltages applied to the stator are constant during the experiments.

III. Experiments

A. Experimental Setup

Fig. 7 shows an experimental setup to measure the position and orientation of the torus wheel. The motion of an AR marker (ArUco3 [28]) on the wheel is captured by a web camera (Logitech Streamcam, 60 fps, 1920×1080 px). A PC analyzes the marker images to calculate the position and orientation. It also sends data on the driving direction of the wheel and the frequency of the applied voltages every 50 ms to a motor driver via a serial communication (Fig. 8). The motor driver applies voltages to the stator via nine enameled wires with a diameter of 0.1 mm, eight of which are soldered to the piezo element and one is connected to the stator for the ground. We use square waves instead of the sine waves shown in (1) to simplify the construction of the motor driver. A planar constraint component, which has two links connected by a pin joint, prevents the tilting of the torus wheel.

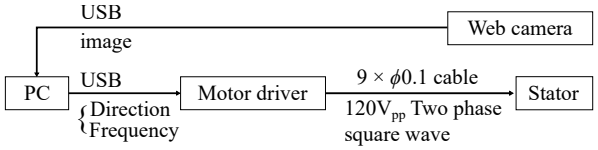

Fig. 8. Control system of the torus wheel for the experimental setup.

B. Longitude and Meridian Movement

To experimentally verify the steady-state velocities V_{l_steady} and V_{m_steady} of the torus wheel in each driving direction, we set four trajectories: positive and negative directions in the longitude and those in the meridian. The wheel moves about 150 mm in each direction five times. Fig.9 (a) shows the wheel trajectories in each driving direction as viewed from the global coordinate system Σ_c. The wheel should have drawn a crisscrossing ideally, but the actual motions have included an unexpected curve. This is because the wheel rotates slightly in the z-axis direction. We use the wheel coordinate system Σ_r, the local coordinate system set to the torus wheel as shown in Fig.7, to ignore rotation in the z-axis direction. Fig.9 (b) shows the wheel trajectories viewed from the wheel coordinate system Σ_r and indicate that the wheel hardly causes errors in angular directions. The angle averages are 353.4 degrees in the positive longitudinal direction, 176.8 degrees in the negative longitudinal direction, 83.4 degrees in the positive meridian direction, and 263.4 degrees in the negative meridian direction. The most probable reason of these angle errors is that the spiral structure of the coil spring depends on the motions of the torus wheel. For example, during the longitudinal motion, the stator accompanies a slight rotation of the coil.

Fig. 10 shows the transient response of the individual wheel velocity in each driving direction, obtained at the experiments in Fig. 9. In this graph, negative curves mean velocities in the negative longitudinal and meridian directions. The velocity in the meridian direction was about 35 mm/s regardless of the positive or negative direction. In the longitudinal direction, the velocities were about 160 mm/s in the positive direction and 120 mm/s in the negative direction. The difference between the positive and negative directions is due to several factors such as fabrication errors of the piezoelectric elements, friction conditions between the stator and the coil, and the flexibility of the torus wheel. The torus wheel suffers from such unstable operating conditions and requires a feedback system for more precise control.

C. Payload Capacity

Because one of main specifications for a mobile robot is its payload capacity, we examine the relationship between the payload and speed of the torus wheel. Fig. 11 shows the speed measured three times each when the loads change from 0 g to 250 g. When the load was 100 g, the speed in the positive longitudinal direction was 60 mm/s, half the no-load speed. The speed in the negative meridian direction was 19 mm/s, half the no-load speed when the load was 140 g. The

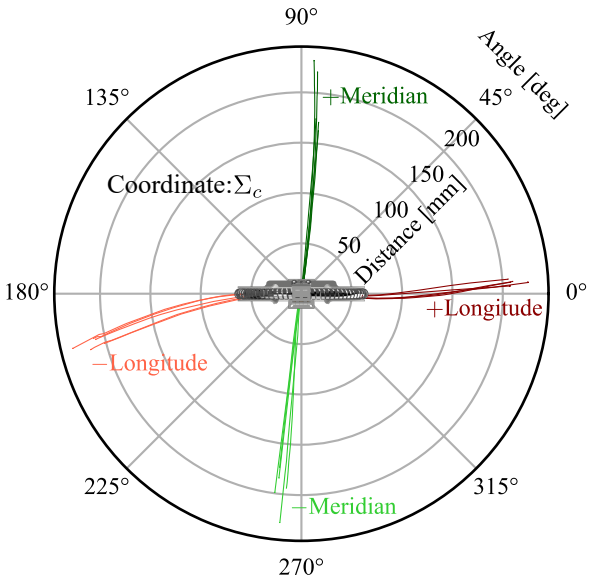

(a)

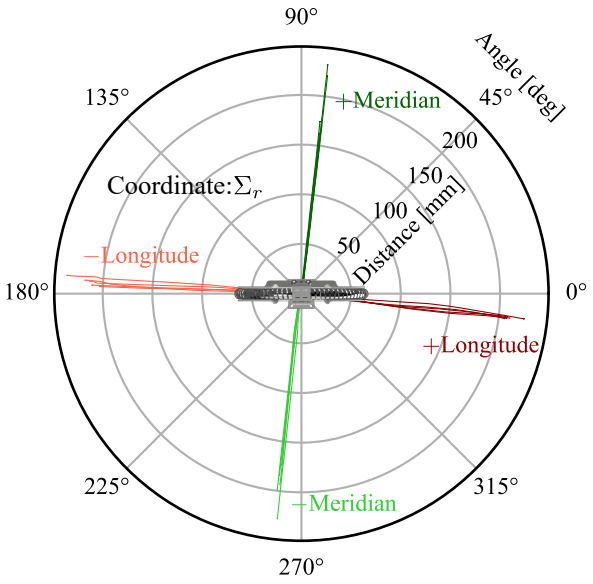

(b)

Fig. 9. Trajectories of the torus wheel when driven in individual longitude and meridian directions. (a) View from the global coordinate system Σ_c. (b) View from the wheel coordinate system Σ_r.

speeds in both directions decrease as the load increases, and the torus wheel can generate little or no motion over a load of 250 g.

From the motion of the robot with the payload, we can estimate the thrust force F and torque τ that the motor generates. When a weight of M_p is placed as the payload to the robot with a weight of M_r, the thrust force that exceeds the static friction in the longitudinal direction is

$$F = \mu_l(M_r + M_p)g \tag{4}$$

where μ_l is the friction coefficient between the coil spring and the housing in the longitudinal direction. As with the thrust force, the torque in the meridian direction is

$$\tau = \mu_m(M_r + M_p)gr \tag{5}$$

where μ_m is the friction coefficient in the meridian direction, and r is the radius of the coil spring. The friction coefficients μ_l = 0.12 and μ_m = 0.09 are obtained experimentally. In the longitudinal direction, the stator performs a thrust force of approximately 195 mN at a speed of 60 mm/s and 379 mN at almost 0 mm/s. In the meridian direction, it shows a torque of approximately 0.937 mNm at 19 mm/s and 1.46 mNm at almost 0 mm/s.

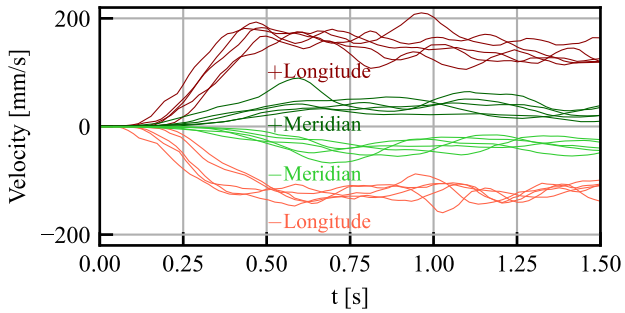

Fig. 10. Velocity of the torus wheel in the longitudinal and meridian directions.

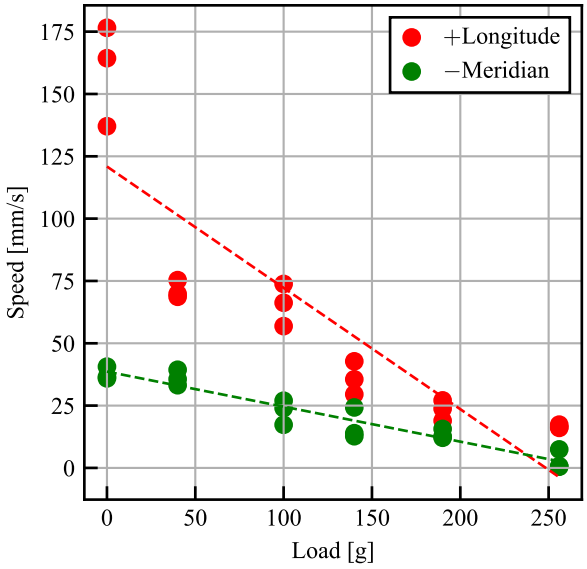

Fig. 11. Relationship between the speed and the payload.

D. Velocity Composition

We verify that the torus wheel can move in all directions by varying the time ratio of the two driving modes per control cycle time T. As shown in Fig.9 (b), the torus wheel causes a slight angular error around z-axis during the individual

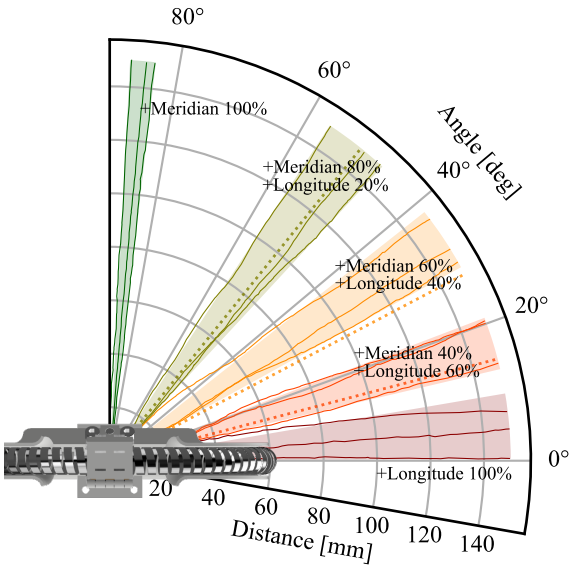

Fig. 12. Composition of longitudinal and meridian velocities.

longitudinal or meridian motion. The theoretical velocites v_x and v_y, taking into account the misalignment around z-axis, are expressed as follows

$$\begin{bmatrix} v_x \\ v_y \end{bmatrix} = \begin{bmatrix} \cos\theta_l & -\sin\theta_m \\ \sin\theta_l & \cos\theta_m \end{bmatrix} \begin{bmatrix} |V_l| \\ |V_m| \end{bmatrix} \tag{6}$$

where θ_l and θ_m are the angles between the ideal and actual paths in individual longitudinal and meridian movements, respectively (counterclockwise is positive).

Fig. 12 shows the wheel trajectories measured three times each when changing the time ratio. The longitudinal and meridian trajectories are slightly different from those in Fig.9 (b). This is due to the unstable operating conditions described in Section III B. The three dotted lines are the theoretical trajectories obtained by substituting the velocities and angles of these trajectories into (2) and (6). The resulting trajectories have been roughly accorded to the theoretical trajectories.

IV. Demonstration

A. Kinematics of Omnidirectional Mobile Robot

We build an omnidirectional mobile robot with two torus wheels and demonstrate its feedback control. Fig. 13 shows a CAD model of the robot, in which the two wheels are placed in parallel with a distance of 80 mm. As in Fig. 7, the AR marker is attached to the robot top to measure the position and orientation. In addition to the robot center coordinate system Σ_r, the coordinate systems of the two torus wheels, Σ_{w0} and Σ_{w1}, are defined. Each torus wheel velocity ${}^{wi}\boldsymbol{v}_{wi} = (v_{wix}, v_{wiy})^T (i = 0, 1)$ when given a desired velocity of the robot ${}^{r}\boldsymbol{v}_r = (v_{rx}, v_{ry}, \omega_{rz})^T$ is

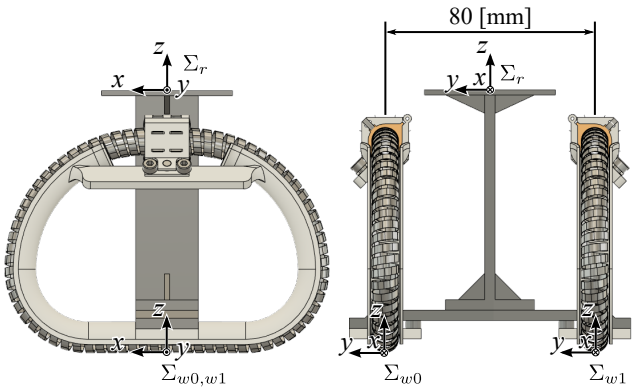

Fig. 13. Omnidirectional mobile robot with two torus wheels.

calculated as follows:

$$\begin{aligned} {}^{wi}\boldsymbol{v}_{wi} &= {}^{r}\boldsymbol{v}_r + {}^{r}\boldsymbol{\omega}_r \times {}^{r}\boldsymbol{P}_{wi} \\ \begin{bmatrix} v_{wix} \\ v_{wiy} \end{bmatrix} &= \begin{bmatrix} 1 & 0 & -P_{wiy} \\ 0 & 1 & P_{wix} \end{bmatrix} \begin{bmatrix} v_{rx} \\ v_{ry} \\ \omega_{rz} \end{bmatrix} (i = 0, 1) \end{aligned} \tag{7}$$

where ${}^{r}\boldsymbol{P}_{wi} = (P_{wix}, P_{wiy}, P_{wiz})^T (i = 0, 1)$ is the Σ_{wi} position viewed from the coordinate system Σ_r.

B. Point-to-point Movement

Omnidirectional mobile robots can move to any place without the path planning that is necessary for existing non-holonomic mobile robots. We demonstrate a holonomic motion of the robot with P control on a plane. The desired position $\boldsymbol{P}_d$ and the present position $\boldsymbol{P}_p$ are composed of three parameters: position x and y in Σ_c and an angle around z-axis in Σ_r. They are given as $\boldsymbol{P}_d = (P_{dx}, P_{dy}, R_{dz})^T$ and $\boldsymbol{P}_p = (P_{px}, P_{py}, R_{pz})^T$. In the controller, the error between $\boldsymbol{P}_d$ and $\boldsymbol{P}_p$ is multiplied by the gain $\boldsymbol{G} = \mathrm{diag}(\mathrm{G_x}, \mathrm{G_y}, \mathrm{G_{rz}})$. The output from the P-controller is applied to the stators as the desired input ($\boldsymbol{G}(\boldsymbol{P}_d - \boldsymbol{P}_p)$). The driving times T_{wil} and T_{wim} that the motor driver applies to the voltages to the wheels can be obtained from (2), (6), and (7) as follows.

$$\begin{aligned} \begin{bmatrix} T_{wil} \\ T_{wim} \end{bmatrix} = \begin{bmatrix} \cos\theta_l & -\sin\theta_m \\ \sin\theta_l & \cos\theta_m \end{bmatrix}^{-1} \Bigg(\begin{bmatrix} 1 & 0 & -P_{wiy} \\ 0 & 1 & P_{wix} \end{bmatrix} \\ (G(\boldsymbol{P}_d - \boldsymbol{P}_p)) \Bigg) \begin{bmatrix} \frac{T}{|V_{l\_steady}|} \\ \frac{T}{|V_{m\_steady}|} \end{bmatrix} \quad (i = 0, 1) \end{aligned} \tag{8}$$

If $T_{wil,wim} < 0$, set $T_{wil,wim} = |T_{wil,wim}|$ and substitute $-\pi/2$ for ϕ in (1) to reverse the stator driving direction. In the case that the sum of the driving times is larger than the control cycle time ($T_{wim} + T_{wil} > T$), the driving times are updated as

$$\begin{bmatrix} T'_{wil} \\ T'_{wim} \end{bmatrix} = \begin{bmatrix} T_{wil} \\ T_{wim} \end{bmatrix} \frac{T}{T_{wil} + T_{wim}} \quad (i = 0, 1) \tag{9}$$

In the experiment, the desired position $\boldsymbol{P}_d$ was set to $(0.1\ \mathrm{m}, 0.1\ \mathrm{m}, 45\ \mathrm{deg})^T$, as shown in Fig. 14. The gain $\boldsymbol{G} =$

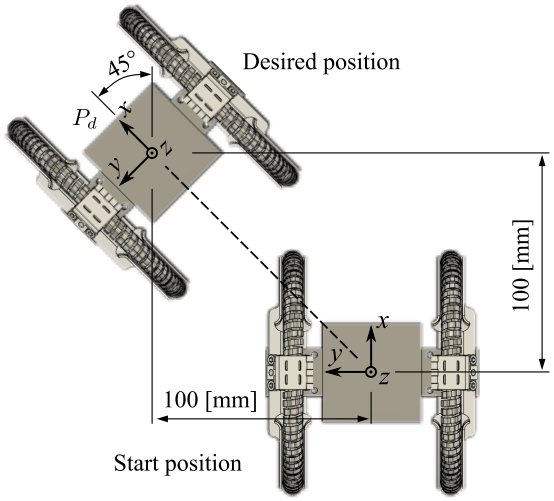

Fig. 14. Point-to-point movement. The robot rotates 45 degrees and moves 100 mm away in both x and y directions.

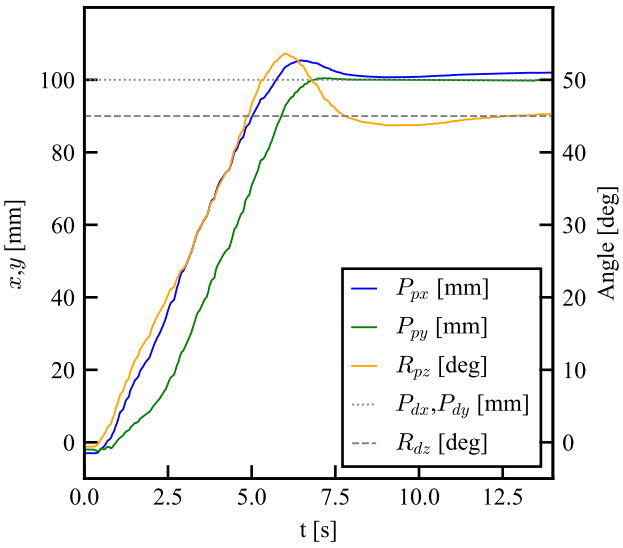

Fig. 15. The transient response of the position and orientation of the robot in point-to-point movement.

$\mathrm{diag}(3, 2, 0.07)$ was obtained experimentally by the marginal sensitivity method. Fig. 15 shows the transient response from the initial position to the desired position. The robot shows the convergence to the desired position P_{dx} and P_{dy} in 8 seconds and the desired angle R_{dz} in 12 seconds.

C. Step Climbing

The housing has been used for the torus made of the flexible coil spring to prevent the deformation of the coil spring. The place that contact the plane is partly flat to increases a contact area for stability, but the flat surface causes a turnover when the robot climbs a step. The flexibility of the coil spring becomes a solution against this problem.

To clarify how the housing shape related to the robot's

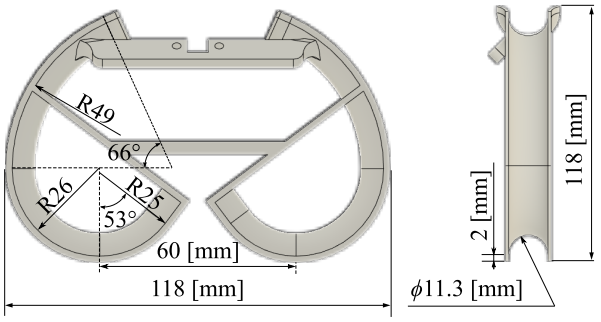

Fig. 16. The housing with a dent that allows deformation of the coil spring for overcoming a step.

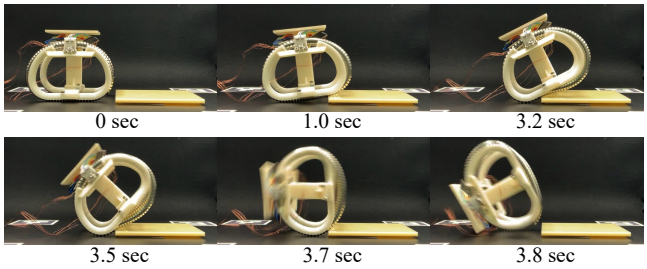

Fig. 17. Snapshots of the robot with the housing without a dent climbing over a step. The robot tilted and fell backward on the step.

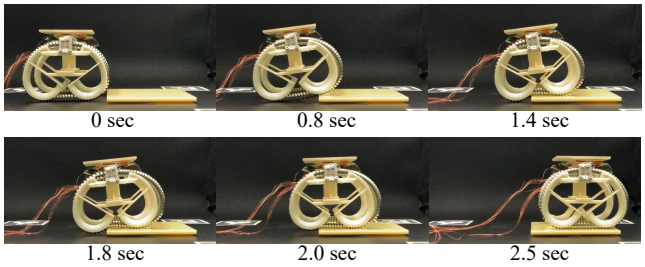

Fig. 18. Snapshots of the robot with the housing with a dent climbing over a step. The robot succeeded in overcoming the step by deforming the wheel to suppress its tilt.

climbing ability, we compare two types of housings, a normal one that is used for the former experiments (Fig. 5) and another one that has a deformability. The deformable one has a dent on the bottom as shown in Fig. 16 while the former forms a flat line on the bottom. This dent allows the torus wheel to deform against an obstacle.

We prepared an 8-mm-height step and compared the robot's climbing behavior with the two housings. Fig. 17 shows a series of snapshots of the robot climbing the step with the normal housing. The robot gradually tilted backward on the step and caused a turnover at 3.7 seconds. Fig. 18 shows that the robot with the deformable wheels climbs the same step. The robot succeeded in climbing the step in 2.0 seconds with almost no tilt due to the compliance of the torus wheel. The limitation of the height that the robot can climb is 8 mm; therefore, it sticks over at higher steps.

V. Conclusions

In this paper, we proposed a palm-sized omnidirectional torus wheel that consists of the piezo-driven stator and the coil spring. The proposed idea is the simplest way that provides omnidirectional mobility to a single wheel without using other components, such as gears, bearings, and transmissions. The torus wheel was able to move at a maximum speed of 160 mm/s in the longitudinal direction and 35 mm/s in the meridian direction. Moreover, the control system showed omnidirectional movement by switching between two driving directions for a short period. The feedback control system was constructed with an original motor driver and a camera. The robot with two torus wheels succeeded in positioning a desired position under P control without a path planning. We created the deformable wheels by modifying the housing design and showed that the robot could overcome an 8 mm step by its compliance.

In our study, there are several points that need to be improved. First, ultrasonic motors that use friction as the driving principle are sensitive to dirt. The proposed robot requires a cleaning mechanism to keep the torus wheel clean or a robust actuation mechanism independent from the dirt. For stable positioning control, an internal sensor used in a feedback loop is required. We are designing a linear variable-resistance sensor to estimate the position of the coil spring. This sensor would be applied to measure the motion of the torus wheel. The proposed stator can be miniaturized into a cube with a side length of 3-4 mm because of its high energy density [29]. With its small size and simple structure, the proposed robot could serve as a low-cost mobile robot platform; for example, it would be useful for swarm robotics, which studies the coordination of multiple robots.

References

[1] T. Takahashi, M. Watanabe, K. Tadakuma, M. Konyo, and S. Tadokoro, "Retraction mechanism of soft torus robot with a hydrostatic skeleton," *IEEE Robotics and Automation Letters*, vol. 5, no. 4, pp. 6900–6907, 2020.

[2] H. Zang, B. Liao, X. Lang, Z.-L. Zhao, W. Yuan, and X.-Q. Feng, "Bionic torus as a self-adaptive soft grasper in robots," *Applied Physics Letters*, vol. 116, no. 2, p. 023701, 2020. [Online]. Available: https://doi.org/10.1063/1.5128474

[3] V. Orekhov, D. W. Hong, and M. Yim, "Actuation mechanisms for biologically inspired everting toroidal robots," in *2010 IEEE/RSJ International Conference on Intelligent Robots and Systems*, 2010, pp. 2535–2536.

[4] E. W. Hawkes, L. H. Blumenschein, J. D. Greer, and A. M. Okamura, "A soft robot that navigates its environment through growth," *Science Robotics*, vol. 2, no. 8, 2017.

[5] T. Abrar, F. Putzu, A. Ataka, H. Godaba, and K. Althoefer, "Highly manoeuvrable eversion robot based on fusion of function with structure," in *2021 IEEE International Conference on Robotics and Automation (ICRA)*. IEEE, 2021, pp. 12 089–12 096.

[6] I. Doroftei, V. Grosu, and V. Spinu, *Omnidirectional mobile robot-design and implementation*. INTECH Open Access Publisher London, UK, 2007.

[7] M. Udengaard and K. Iagnemma, "Analysis, design, and control of an omnidirectional mobile robot in rough terrain," *ASME Journal of Mechanical Design*, vol. 131, no. 12, 2009.

[8] H. Taheri and C. X. Zhao, "Omnidirectional mobile robots, mechanisms and navigation approaches," *Mechanism and Machine Theory*, vol. 153, p. 103958, 2020.

[9] C. Chen, S. Ostrovskaya, and J. Angeles, "The kinematics of wheeled mobile robots with dual-wheel transmission units," *Journal of Mechanical Design*, vol. 130, no. 1, 2008.

[10] J. GRABOWIECKI, "Vehicle-wheel," 1919, uS Patent no1,305,535.

[11] I. Paromtchik, H. Asama, T. Fujii, and L. Endo, "A control system for an omnidirectional mobile robot," in *Proceedings of the 1999 IEEE International Conference on Control Applications (Cat. No. 99CH36328)*, vol. 2. IEEE, 1999, pp. 1123–1128.

[12] S. Ganapathy, "Decomposition of transformation matrices for robot vision," *Pattern Recognition Letters*, vol. 2, no. 6, pp. 401–412, 1984.

[13] D. B. Harris, "Low vibration omni-directional wheel," Jan. 22 2002, uS Patent 6,340,065.

[14] D. Chugo, K. Kawabata, H. Kaetsu, H. Asama, and T. Mishima, "Development of a control system for an omni-directional vehicle with step-climbing ability," *Advanced Robotics*, vol. 19, no. 1, pp. 55–71, 2005.

[15] S. Hirose, "The vuton: High payload high efficiency holonomic omni-directional vehicle," *Proc. ISRR, Hidden Valley, USA, 1993*, pp. 253–260, 1993.

[16] K. Tadakuma, R. Tadakuma, K. Nagatani, K. Yoshida, S. Peters, M. Udengaard, and K. Iagnemma, "Crawler vehicle with circular cross-section unit to realize sideways motion," in *2008 IEEE/RSJ International Conference on Intelligent Robots and Systems*. IEEE, 2008, pp. 2422–2428.

[17] J. T. Lane and R. M. Voyles, "A 2-d tread mechanism for hybridization in usar robotics," in *2015 IEEE International Symposium on Safety, Security, and Rescue Robotics (SSRR)*. IEEE, 2015, pp. 1–6.

[18] J. Huff, S. Conyers, and R. Voyles, "Mothership—a serpentine tread/limb hybrid marsupial robot for usar," in *2012 IEEE International Symposium on Safety, Security, and Rescue Robotics (SSRR)*. IEEE, 2012, pp. 1–7.

[19] K. Tadakuma, E. Takane, M. Fujita, A. Nomura, H. Komatsu, M. Konyo, and S. Tadokoro, "Planar omnidirectional crawler mobile mechanism—development of actual mechanical prototype and basic experiments," *IEEE Robotics and Automation Letters*, vol. 3, no. 1, pp. 395–402, 2017.

[20] U. Nagarajan, G. Kantor, and R. Hollis, "The ballbot: An omnidirectional balancing mobile robot," *The International Journal of Robotics Research*, vol. 33, no. 6, pp. 917–930, 2014.

[21] M. Kumagai and T. Ochiai, "Development of a robot balancing on a ball," in *2008 International Conference on Control, Automation and Systems*. IEEE, 2008, pp. 433–438.

[22] "Murata cheerleaders," 2022, https://corporate.murata.com/en-us/more_murata/robots/mcheerleaders.

[23] W.-H. Chen, C.-P. Chen, J.-S. Tsai, J. Yang, and P.-C. Lin, "Design and implementation of a ball-driven omnidirectional spherical robot," *Mechanism and Machine Theory*, vol. 68, pp. 35–48, 2013.

[24] A. Kanada and T. Mashimo, "Design and experiments of flexible ultrasonic motor using a coil spring slider," *IEEE/ASME Transactions on Mechatronics*, vol. 25, no. 1, pp. 468–476, 2019.

[25] Y. Sato, A. Kanada, and T. Mashimo, "Self-sensing and feedback control for a twin coil spring-based flexible ultrasonic motor," *IEEE Robotics and Automation Letters*, vol. 5, no. 4, pp. 5425–5431, 2020.

[26] H. Makino, "Frictional drive device and inverted pendulum type vehicle using the same," Apr. 2 2013, US Patent 8,408,339.

[27] W. Liddiard, "Omnidirectional wheel," Sep. 26 2017, US Patent 9,770,943.

[28] F. Romero-Ramirez, R. Muñoz-Salinas, and R. Medina-Carnicer, "Speeded up detection of squared fiducial markers," *Image and Vision Computing*, vol. 76, 06 2018.

[29] T. Mashimo and S. Toyama, "Rotary-linear piezoelectric microactuator with a cubic stator of side length 3.5 mm," *IEEE transactions on ultrasonics, ferroelectrics, and frequency control*, vol. 57, no. 8, pp. 1825–1830, 2010.